PHYSICAL REVIEW B VOLUME 57, NUMBER 4 15 JANUARY 1998-II

Electronic structure of electron doped $SrTiO_3$: $SrTiO_{3-\delta}$ and $Sr_{1-x}La_xTiO_3$

N. Shanthi and D. D. Sarma*
Solid State and Structural Chemistry Unit, Indian Institute of Science, Bangalore 560012, India

(Received 13 June 1997)

Electronic structures of electron-doped $SrTiO_{3-\delta}$ and $Sr_{1-x}La_xTiO_3$ have been investigated within the *ab initio* band-structure approach using a supercell containing eight basic units. A small amount of electron doping is found to drive $SrTiO_3$ metallic, with the Fermi level moving into the conduction band in both the systems. Clustering of oxygen vacancies in the case of $SrTiO_{3-\delta}$ gives rise to distinct non-rigid-band-like evolution of the electronic structure, trapping doped charge carriers in midgap states; similar effects are not observed for $Sr_{1-x}La_xTiO_3$, explaining the difference in the Hall measurements of these two closely related compounds. [S0163-1829(98)01404-0]

INTRODUCTION

Stoichiometric $SrTiO_3$ with Ti^{4+} ions has a d^0 electron configuration, and consequently is a band insulator[1] with a band gap of about 3.2 eV. It is a well-known ferroelectric material[2] with a wide range of technological applications. It is also used as a substrate material for growing thin films. Thus its electronic and other properties have been extensively studied over the years.[3–7] In recent years, there has been a renewed interest in the electronic structure of $SrTiO_3$ doped with charge carriers (electrons).[8–11] Such electron doping is known to transform insulating $SrTiO_3$ readily into a metallic state even with a very small extent of doping. Doping can be achieved by altering any of the three sublattices, namely, those of Sr, Ti, and O. Specifically, La substitution[11–13] at the Sr site ($Sr_{1-x}La_xTiO_3$) and vacancies at the oxygen sites ($SrTiO_{3-\delta}$) (Refs. 3–10) dope electrons into the system, and have been extensively studied in the past. Not only does this system undergo an insulator-to-metal transition on doping, it has been reported that the compounds even become superconducting at low temperatures ($T_c<0.3$ K) for a range of compositions. The extensively studied systems, $Sr_{1-x}La_xTiO_3$ and $SrTiO_{3-\delta}$, have many similarities. For example, in both cases an insulator to metal transition takes place for an extremely small number[6,8,11,14] of electron doping (on the order of 10^{19} cm^{-3}). The highest T_c for the superconducting transition is about 0.3 K for both systems. In spite of these similarities there are some specific differences between these two closely related systems. It has been found[13] that there is exactly one delocalized electron doped for every atomic substitution of Sr by La in $Sr_{1-x}La_xTiO_3$; in other words, there are x number of electrons per Ti site in this series. It is to be noted that in the case of oxygen vacancies, $SrTiO_{3-\delta}$ is expected to have 2δ number of electrons doped for every formula unit. In contrast, Hall measurements[15] suggest that there are only $\delta/2$ number of conduction electrons in $SrTiO_3$ for larger values of δ (≈ 0.28). Thus 75% of the doped electrons do not appear as charge carriers or contribute to the conduction process in such cases. The discrepancy between the number of charge carriers found experimentally, and that expected on the basis of the chemical formula, tend to decrease with decreasing δ or nonstoichiometry.

In order to understand such unexpected differences in the electronic structures of differently doped $SrTiO_3$ compounds, we investigated $Sr_{1-x}La_xTiO_3$ and $SrTiO_{3-\delta}$ in terms of *ab initio* band-structure calculations. It is known that strong electron-electron interaction effects often make the effectively one-electron band structure approaches seriously inadequate for a large number of transition-metal compounds. However, $SrTiO_3$ has a d^0 configuration and, thus, is a band insulator rather than being a correlated (Mott) insulator. In such cases, *ab initio* band-structure results are known[16] to be reliable. Even in the doped cases, there are very few electrons ($\ll 1$) per Ti site in the system. This ensures that the effect of electron correlation on the elctronic structure is not very important, also making *ab initio* band-structure methods a good starting point for describing the electronic structure of the doped systems. The results obtained here establish that there are indeed important differences in the doping-dependent evolution of the electronic structure in the two systems, $Sr_{1-x}La_xTiO_3$ and $SrTiO_{3-\delta}$, though both represent electron doping of the empty conduction band in $SrTiO_3$. Specifically, though the modifications in the density of states with La substitution can be described within a rigid-band model, the changes in the density of states (DOS) of $SrTiO_{3-\delta}$ with changing δ cannot at all be explained with such a model.

METHOD OF CALCULATION

$SrTiO_3$ is possibly the best-known example of the cubic perovskite[17] with the space group $Pm3m$, where Ti atoms are at cube corners, Sr atoms at cube centers, and O atoms at edge centers. The unit cell contains one formula unit of $SrTiO_3$. In order to study fractional oxygen vacancy (or La substitution) in each formula unit, it is necessary to consider a larger cell than the basic unit. Thus we have constructed a supercell of eight unit cells consisting of 40 atoms in the basis. We study the oxygen deficiency by replacing oxygen atoms in this supercell by empty spheres. Replacing any one of the oxygens in the supercell will correspond to the formula $SrTiO_{2.875}$ or $SrTiO_{3-\delta}$ with $\delta=0.125$. Having two vacancies will correspond to the formula $SrTiO_{2.75}$ with $\delta=0.25$. In the case of a single vacancy in the supercell, there is no difference between configurations with the vacancy at

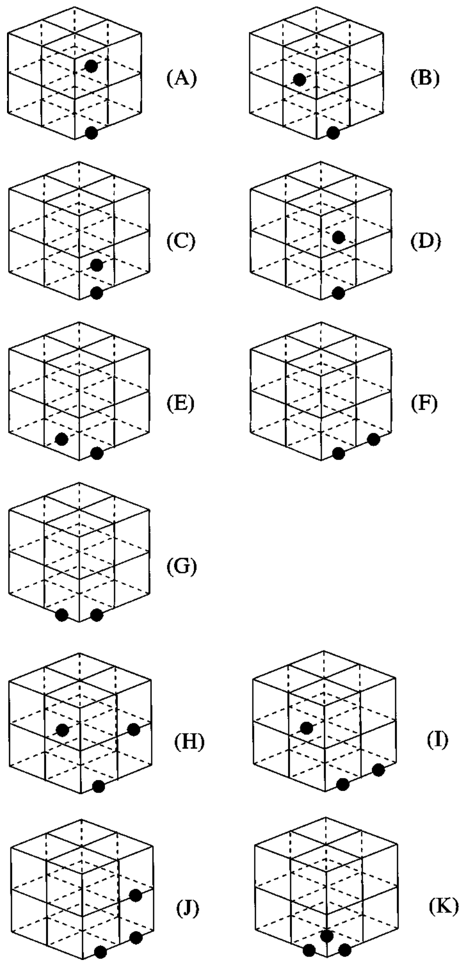

FIG. 1. Different configurations arising from the distribution of two oxygen vacancies in the supercell ($A-G$). Some of the distinct configurations arising from the distribution of three oxygen vacancies in the supercell ($H-K$). Only the vacancy positions are indicated by solid circles.

different oxygen sites in the cell; all such configurations are equivalent. However, the situation becomes complicated with two vacancies in the supercell. There are seven different ways of distributing the two vacancies in the supercell, distinguished from each other by the relative positions of the two vacancies, and each configuration leads to a unique electronic structure. These seven distinct configurations ($A-G$) are shown in Fig. 1 with decreasing vacancy-vacancy separation; the distance between the two vacancies corresponding to each configuration is tabulated in Table I. We have studied all of these configurations. There are many distinct configurations possible with three oxygen vacancies in the supercell corresponding to the chemical formula $SrTiO_{2.625}$; we have investigated only four representative configurations [Fig. 1] in this case. These include configuration H, where all the three oxygen vacancies are farthest apart from each other; configurations I and J, where two out of three vacancies are nearer to each other; and configuration K, with all three vacancies closest to each other. We have also studied the lanthanum doped compositions ($Sr_{1-x}La_xTiO_3$) by replacing Sr with La in the supercell. In this case, we have studied the compositions $Sr_{0.875}La_{0.125}TiO_3$, $Sr_{0.75}La_{0.25}TiO_3$, and $Sr_{0.625}La_{0.375}TiO_3$ by replacing 1, 2, and 3 Sr, respectively, by La in the supercell. In each of the latter two cases (two- and three-atom substitutions), two distinct configurations were studied with the substituent atoms closest to and farthest from each other. In undoped $SrTiO_3$ all atoms of the same type, Sr, Ti, or O, in the unit cell are equivalent. However, in the presence of doping or vacancy, the translational symmetry within the supercell is broken and the various atoms of the same type become inequivalent.

TABLE I. Distance between the two oxygen vacancies in $SrTiO_{2.75}$.

Configurations	Distance between the vacancies
A	$\sqrt{3}a$
B	$\sqrt{2}a$
C	$\sqrt{2}a$
D	$\sqrt{3/2}a$
E	a
F	a
G	$a/\sqrt{2}$

We have used the linearized muffin-tin orbital method within the atomic-sphere approximation[18] (LMTO-ASA) to study all of the above-mentioned configurations. No effort was made to optimize the structure within these calculations, since the supercell approach becomes computationally prohibitive particularly in view of the large number of different configurations involved. However, it is known that the crystal structure and the lattice parameters do not vary significantly for small dopings in $SrTiO_3$.[15] Self-consistency was acheived with 216 k points in the Brillouin zone, and with s, p, and d bases within each atomic sphere. The energies E_ν^l for each angular momentum partial wave were chosen at the center of gravity of the occupied parts of the corresponding partial DOS. The contribution of the vacancy states to the density of states was obtained by adding different angular momentum components corresponding to the empty sphere considered at the vacancy site.

RESULTS AND DISCUSSION

We show the total DOS for stoichiometric $SrTiO_3$ in Fig. 2(a). The total DOS in this energy range is almost entirely contributed by the partial densities of states (PDOS) for Ti d and O p states, also shown in the figure. The results clearly exhibit a band gap of about 2.5 eV. The calculated band gap is somewhat less than the experimentally observed gap of 3.2 eV. Such an underestimation of the band gap is a well-known limitation of the local-density approximation,[19] which treats the electron exchange correlation in an approximate way. The occupied part of the DOS is made up predominantly of the O p PDOS, consistent with $SrTiO_3$ being a formal d^0 system with the valency of Ti as 4+. However, there is a finite Ti d PDOS in the occupied energy range due to the hybridization with the O p states. There are basically two groups of features around -5.5 and -3.5 eV. The Ti d PDOS contribution is maximum in the vicinity of -5.5 eV, suggesting that these states arise primarily from bonding interactions between the O p and Ti d states. The Ti d PDOS

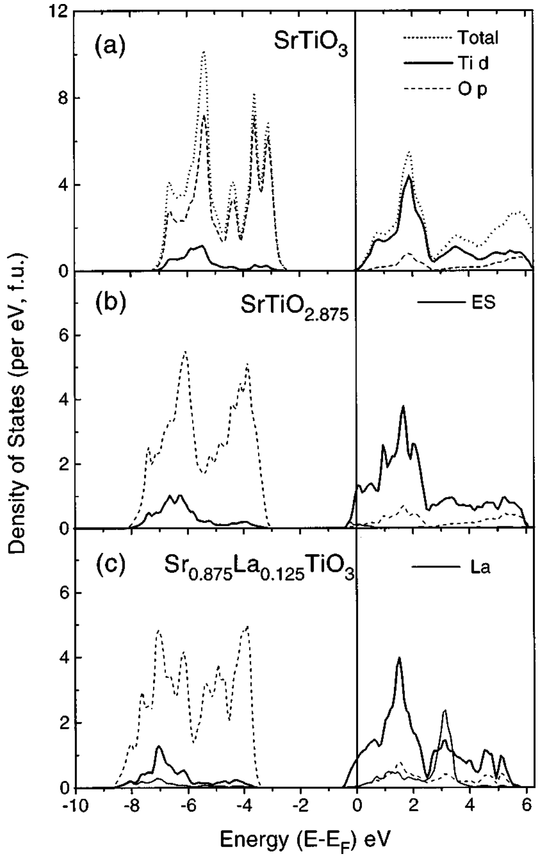

FIG. 2. (a) Total DOS (dotted line), Ti *d* PDOS (solid line), and O *p* PDOS (dashed line) in $SrTiO_3$. (b) PDOS of Ti *d*, O *p*, and total contribution from the empty sphere (ES) (thin solid line) in $SrTiO_{2.875}$. (c) PDOS of Ti *d*, O *p*, and total from La (thin solid line) of $Sr_{0.875}La_{0.125}TiO_3$.

is very weak in the vicinity of -3.5 eV features in the O *p* PDOS; therefore we attribute the features in this energy range to be arising primarily from O *p*–O *p* interactions with a nonbonding character with respect to O *p*–Ti *d* interactions. The unoccupied DOS shown in Fig. 2(a) is dominated by Ti *d* PDOS with small contributions from O *p* PDOS. Thus the conduction band of this band insulator has primarily Ti *d* character. Any electron doped into this material is expected to occupy the bottom of these bands, shifting the Fermi energy into the conduction band and consequently giving the system a metallic ground state. In the following, we concentrate on the changes in the electronic structure of $SrTiO_3$ on doping with electrons.

Results for $SrTiO_{2.875}$, which corresponds to one of the oxygen atoms in the supercell being replaced by an empty sphere, and therefore donating 0.25 electrons per formula unit, is shown in Fig. 2(b). For the sake of clarity, we do not show the total DOS here and in the subsequent figures, and only the relevent Ti *d* and O *p* PDOS along with the PDOS arising from states in the empty sphere, are shown. The total DOS in the energy range of interest is almost entirely made of these states. While the overall PDOS features remain approximately similar to those of $SrTiO_3$ [Fig. 2(a)], the Fermi energy in this case moves inside the conduction band, in agreement with the metallic ground state of such compositions as a consequence of electron doping. The occupied states at the bottom of the conduction band have primarily Ti *d* character, though there also is a non-negligible contribution to these states from the empty spheres. The changes in the DOS due to the smallest extent of electron doping studied in this work, as shown in Fig. 2(a), can be described approximately in terms of essentially a rigid-band shift of the Fermi energy within the conduction band due to the doping of electrons.

Figure 2(c) shows the partial DOS in the case where one La substitutes for one of the Sr atoms in the supercell, corresponding to the formula $Sr_{0.875}La_{0.125}TiO_3$. As expected, the Fermi energy moves into the conduction band due to electron doping, and the band structure corresponds to a metallic state, in agreement with experimental observations. The overall electronic structures shown in Fig. 2(b) and 2(c) are similar due to the underlying phenomenon of electron doping of the band insulator in both cases. There are, however, some differences in details that can be observed. In the case of La substitution, primarily O *p*-derived states appearing far below E_F are somewhat more modified from the parent $SrTiO_3$ features than that in the case of oxygen vacancies. Since La-derived states (primarily La *d* PDOS) appear with non-negligible density in this energy range, it is clear that these redistributions within the primarily oxygen *p* band arises from hybridization mixing with such La-derived states. Moreover, La-derived states do not contribute states close to E_F, since the basic electronic structure responsible for the transport properties in these materials are almost entirely dominated by Ti *d*–O *p* interactions, via the three-dimensional network of corner-shared TiO_6 octahedra. In contrast, an oxygen vacancy is found to make a more significant contribution at and near the Fermi energy, as shown by the finite contributions of the empty sphere in this energy region [Fig. 2(b)], since oxygen vacancies directly influence the fundamental interactions of the electronic structure by disrupting the Ti-O network. However, these small changes in the DOS and PDOS shown in Figs. 2(b) and 2(c) do not explain the fundamentally different behaviors of the two types of electron doping of $SrTiO_3$, as indicated by Hall measurements.[13,15]

In subsequent discussions on the effect of oxygen vacancies, we restrict ourselves to the states near E_F which control the physical properties of these systems. In Fig. 3 (curves $A-G$), we show Ti *d*, O *p*, and the empty-sphere contributions to the DOS of $SrTiO_{2.75}$ with two oxygen vacancies in the supercell. These panels are arranged according to the decreasing separation between the two vacancies, and the corresponding supercells are shown in Fig. 1. When the oxygen vacancies are farthest apart (curve A), the Fermi energy is found to shift further into the conduction band, accounting for twice the electron doping compared to $SrTiO_{2.875}$ [Fig. 2(b)]. There is substantial amount of contributions from the empty-sphere states close to E_F, though the Ti *d* PDOS dominates over most of the energy region. The change in the electronic structure for this configuration is still describable within a rigid-band description. As the two vacancies move closer (curves B and C), there is however a distortion near the bottom of the conduction band, with the PDOS showing a distinct tailing to energies further below E_F, as indicated by the arrows in the figures. This is an indication of an incipient localization of some of the doped electrons being trapped by the oxygen vacancies. This is further supported

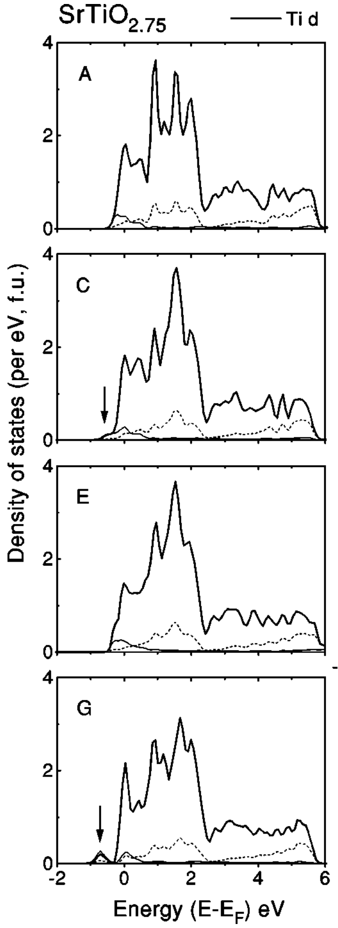

FIG. 3. PDOS of Ti *d* (solid line), O *p* (dashed line), and total ES (thin solid line) in $SrTiO_{2.75}$ for the configurations shown in Fig. 1. The vertical arrows point to the distortions near the bottom of the conduction band, leading to the formation of midgap states with decreasing vacancy-vacancy separation or increasing oxygen clustering.

by the fact that the empty-sphere contribution precisely over this range of energies is as much as that from Ti *d* states. This effect is further accentuated, and made evident, when the two oxygen vacancies are brought closer together (marked by arrows in curves *F* and *G*). In these two cases, there are states pulled from the bottom of the conduction band far below E_F into the midgap region. In curve *G*, these states are even separated from the remaining part of the conduction band, with a small but finite gap. In these cases, it is clear that the contribution from the empty spheres at the oxygen vacancies is substantial, suggesting that the vacancy potentials play an important role in forming such midgap localized states. It also appears necessary to have the vacancies close together on the same TiO_6 octahedra [see configurations *F* and *G* in Fig. 1] for such effects to show up prominently. It is not enough to have the vacancies nearby, but on different TiO_6 units. For example, in configurations *E* and *F*, the two vacancies are equally far apart (Table I). In configuration *E*, however, the two vacancies belong to two different TiO_6 octahedra in contrast to configuration *F*, and, consequently, only in the case of *F* does one see the formation of deep midgap states. In other words, it is necessary for the vacancies to cluster together in order to localize electron states in the midgap region. It is obvious from the results that the changes in the density of states due to such vacancy clustering is distinctly non-rigid-band-like. It is to be noted that these localized states have substantial Ti *d* character along with the empty-sphere contributions, indicating that the electrons are localized on Ti and the vacancy sites.

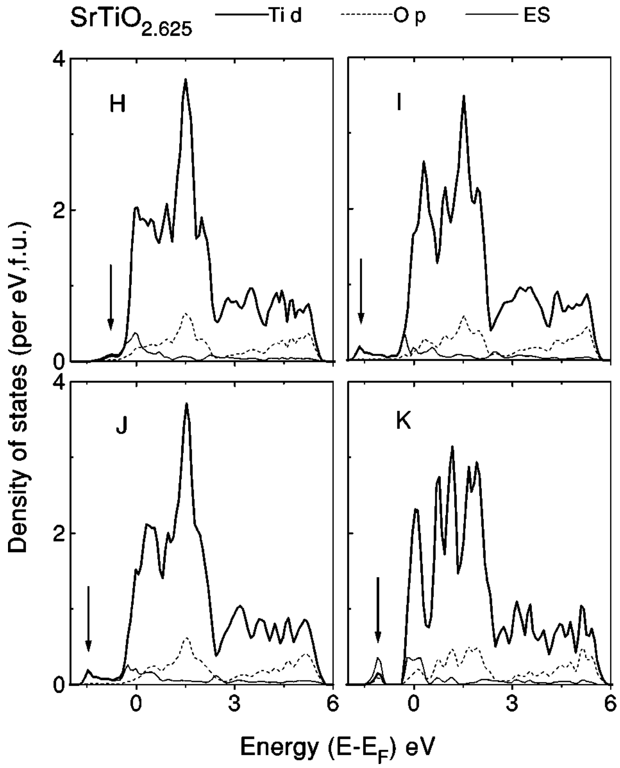

FIG. 4. PDOS of Ti *d* (solid line), O *p* (dashed line), and total ES (thin solid line) in $SrTiO_{2.625}$ for the configurations shown in Fig. 1. The vertical arrows point to the distortions near the bottom of the conduction band leading to the formation of midgap states with decreasing vacancy-vacancy separation or increasing oxygen clustering.

Very similar trends are further accentuated (as indicated by the arrows in the figure), with three oxygen vacancies in the supercell corresponding to a chemical formula of $SrTiO_{2.625}$. PDOS's corresponding to the different configurations shown in Fig. 1 are given in the corresponding curves of Fig. 4. When the three vacancies are farthest apart, on three different TiO_6 octahedra (curve *H*), the bottom of the conduction band shows a distinct distortion extending the states to nearly -1.5 eV below E_F. In the intermediate situation with two vacancies on the same TiO_6 unit with the third vacancy on a different one, the midgap states are clearly defined with some low density of states connecting them to the bottom of the conduction band (curves *I* and *J*). In the opposite extreme of all the three vacancies on the same TiO_6 unit (curve *K*), the midgap states are completely localized and separated from the conduction band with a substantial gap of about 0.5 eV. In every case, the empty-sphere contributions dominate in these states pulled below the conduction band into the midgap region, though the Ti *d* PDOS also contributes significantly. In contrast, the states near the Fermi energy are always dominated by Ti *d* PDOS.

It is clear that such midgap states localized due to vacancy clustering will not contribute to the transport properties of the sample. In other words, only a part of the electrons doped by the presence of oxygen vacancies will be available for conduction and be seen by Hall measurements, while a substantial part will remain localized. However, our results also suggest that a vacancy clustering is essential for such trapping of the doped electrons, and homogeneously distributed vacancies do not give rise to any localization. In this context, it is interesting to note that extensive vacancy clustering has indeed been observed on the surface of oxygen-deficient $SrTiO_{3-\delta}$.[20] Thus it is tempting to speculate that a similar clustering of vacancies may also be taking place in the bulk of these samples; this possibility can be probed by the transmission electron microscope. It is, however, clear that our results provide an explanation for the unusual Hall results[15] in terms of vacancy clustering in the bulk of $SrTiO_{3-\delta}$. The present results also suggest a reason for the observation[15] that the discrepancy between the number of electrons doped chemically (2δ in $SrTiO_{3-\delta}$) and the number measured by Hall experiments decreases with decreasing oxygen vacancies (δ). In the very dilute limit, the oxygen vacancies remain separated, and do not lead to clustering. The present results show that no split-off localized states form in such situations and the effect is describable in terms of a rigid shift of the Fermi energy. With increasing vacancy concentration, more extensive clustering takes place, leading to the localization of the doped electrons.

In order to understand the different behavior of La-substituted samples, $Sr_{1-x}La_xTiO_3$ compared to $SrTiO_{3-\delta}$, we studied some representative configurations with La occupying some of the Sr sites in the supercell, and the results are shown in Fig. 5. We show the results for two and three La atoms in the supercell corresponding to the chemical formula $Sr_{0.75}La_{0.25}TiO_3$ and $Sr_{0.625}La_{0.375}TiO_3$, respectively, in Fig. 5. In each of the two cases, we study two configurations with the La atoms farthest apart [Figs. 5(a) and 5(c)] and closest together [Figs. 5(b) and 5(d)]. The results for the two La atoms in the supercell $Sr_{0.75}La_{0.25}TiO_3$ show a further movement of the Fermi energy into the conduction band compared to $Sr_{0.875}La_{0.125}TiO_3$ [Fig. 2(b)] to accommodate the increased number of doped electrons. Besides this change, the results, particularly those related to the conduction-band states, are remarkably similar for one- [Fig. 2(c)] and two- and three-atom (Fig. 5) substitutions irrespective of whether the La atoms are close together or remain far apart. In particular, there is no tendency for the formation of midgap states in this case, in sharp contrast to the case of $SrTiO_{3-\delta}$; instead, the results here are consistent with a rigid-band description of electron doping in a band insulator. This is in agreement with the experimental observation[13] that the number of conduction electrons estimated by Hall measurements agrees well with the number of doped electrons according to the chemical formula $Sr_{1-x}La_xTiO_3$.

In conclusion, we investigated electronic structures of electron-doped $SrTiO_{3-\delta}$ and $Sr_{1-x}La_xTiO_3$ for several values of δ and x, and different geometric arrangements of the oxygen vacancies / La substituents. *Ab initio* band structure calculations using LMTO-ASA method on a supercell containing eight formula units of $SrTiO_3$ were performed to understand the basic differences in the electronic structure of these two closely related systems. It is found that electron doping in the case of $Sr_{1-x}La_xTiO_3$ can be described fairly well within a rigid-band model, where the Fermi energy progressively shifts into the conduction band with doping. This shows that every electron doped into the system contributes to the conduction process. At low vacancy concentration, the electronic structure of $SrTiO_{3-\delta}$ resembles that of $Sr_{1-x}La_xTiO_3$. With incresing δ, however, it is found that vacancy clustering seriously distorts the bottom of the conduction band, making it impossible to describe the evolution of the DOS even approximately within the rigid-band model. Several configurations of the vacancy clustering lead to the formation of localized midgap states in $SrTiO_{3-\delta}$. Thus only a part of the electrons doped contributes to the conduction process, with a sizable portion being trapped by the vacancy clusters. These results are consistent with Hall measurements on these compounds.[13,15]

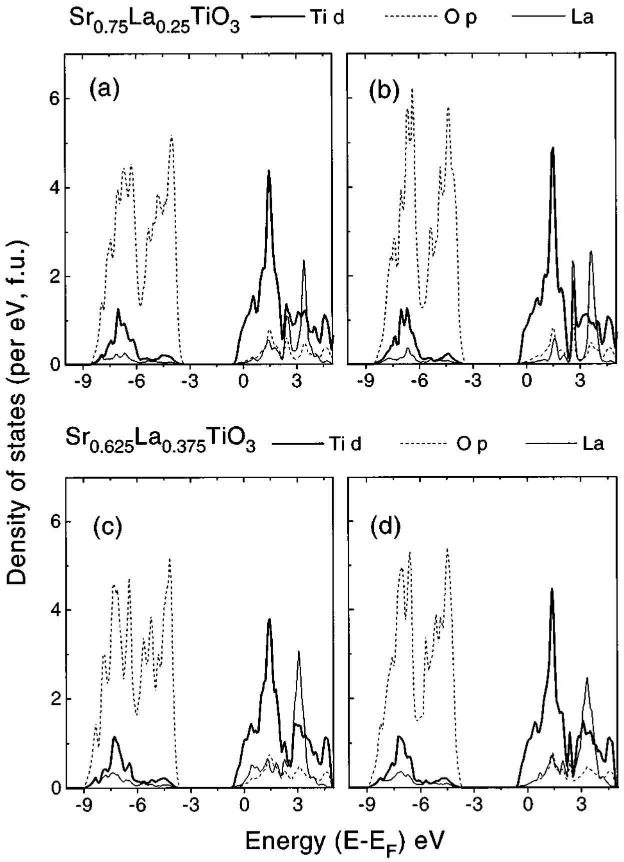

FIG. 5. PDOS of Ti *d* (solid line), O *p* (dashed line), and total La (thin solid line) in $Sr_{1-x}La_xTiO_3$. (a) For $x=0.25$, with the two La atoms farthest apart from each other. (b) For $x=0.25$, with the two La atoms closest to each other. (c) For $x=0.375$, with the three La atoms farthest apart. (d) For $x=0.375$, with the three La atoms closest to each other.

ACKNOWLEDGMENTS

We thank Dr. M. Methfessel, Dr. A.T. Paxton, and Dr. M. van Schiljgaarde for making the LMTO-ASA band-structure program available, and Dr. S. Krishnamurthy for initial help in setting up the LMTO-ASA program. N.S. is thankful to Dr. S.R. Barman for helpful discussions and CSIR, government of India, for financial support.

[*] Also at Jawaharlal Nehru Center for Advanced Scientific Research, Bangalore, India. Electronic address: sarma@sscu.iisc.ernet.in

[1] M. Cardona, Phys. Rev. **140**, A651 (1965).

[2] H. E. Weaver, J. Phys. Chem. Solids **11**, 274 (1959).

[3] J. F. Schooley, W. R. Hosler, and M. L. Cohen, Phys. Rev. Lett. **12**, 474 (1964).

[4] H. P. R. Ferderikse, W. R. Thurber, and W. R. Hosler, Phys. Rev. **134**, A442 (1964).

[5] O. N. Tufte and P. W. Chapman, Phys. Rev. **155**, 796 (1967).

[6] C. S. Koonce, M. L. Cohen, J. F. Schooley, W. R. Hosler, and E. R. Pfeiffer, Phys. Rev. **163**, 380 (1967).

[7] C. Lee, J. Yahia, and J. L. Brebner, Phys. Rev. B **3**, 2525 (1971).

[8] P. Calvani, M. Capizzi, F. Donato, S. Lupi, P. Maselli, and D. Peschiaroli, Phys. Rev. B **47**, 8917 (1993).

[9] Y. Haruyama, H. Fukutani, Y. Aiura, Y. Nishihara, T. Komeda, S. Kodaira, T. Maruyama, and H. Kato, Jpn. J. Appl. Phys., Part 1 **32**, 543 (1993).

[10] D. D. Sarma, S. R. Barman, H. Kajueter, and G. Kotliar, Europhys. Lett. **36**, 307 (1996).

[11] H. Suzuki, H. Bando, Y. Ootuka, I. H. Inoue, T. Yamamoto, K. Takahashi, and Y. Nishihara, J. Phys. Soc. Jpn. **65**, 1529 (1996).

[12] A. Fujimori, I. Hase, M. Nakamura, H. Namatame, Y. Fujishima, Y. Tokura, M. Abbate, F. M. F. de Groot, M. J. Czyzyk, J. C. Fuggle, O. Strebel, F. Lopez, M. Domke, and G. Kaindl, Phys. Rev. B **46**, 9841 (1992).

[13] Y. Tokura, Y. Taguchi, Y. Okada, Y. Fujishima, T. Arima, K. Kumagai, and Y. Iye, Phys. Rev. Lett. **70**, 2126 (1993).

[14] C. Lee, J. Destry, and J. L. Brebner, Phys. Rev. B **11**, 2299 (1975).

[15] W. Gong, H. Yun, Y. B. Ning, J. E. Greedan, W. R. Datans, and C. V. Stager, J. Solid State Chem. **90**, 320 (1991).

[16] D. D. Sarma, N. Shanthi, S. R. Barman, N. Hamada, H. Sawada, and K. Terakura, Phys. Rev. Lett. **75**, 1126 (1995).

[17] F. S. Galasso, *Structure and Properties of Inorganic Solids* (Pergamon, Oxford, 1970), p. 179.

[18] O. K. Anderson, Phys. Rev. B **12**, 3060 (1975); H. L. Skriver, *The LMTO Method* (Springer, Berlin, 1984).

[19] W. K. Pickett, Rev. Mod. Phys. **61**, 433 (1989).

[20] Y. Aiura, H. Bando, Y. Nishihara, Y. Haruyama, S. Kodaira, T. Komeda, Y. Sakisaka, T. Maruyama, and H. Kato, in *Advances in Superconductivity VI*, edited by T. Fujita and Y. Shiohara (Springer-Verlag, Tokyo, 1994).